



# Linoleic acid improves PIEZO2 dysfunction in a mouse model of Angelman Syndrome

Received: 3 October 2022

Accepted: 17 February 2023

Published online: 01 March 2023

Check for updates

Luis O. Romero , Rebeca Caires , A. Kaitlyn Victor<sup>3</sup>, Juanma Ramirez<sup>4</sup>, Francisco J. Sierra-Valdez , Patrick Walsh<sup>6</sup>, Vincent Truong<sup>6</sup>, Jungsoo Lee , Ugo Mayor , Lawrence T. Reiter<sup>3,8,9</sup>, Valeria Vásquez & Julio F. Cordero-Morales

Angelman syndrome (AS) is a neurogenetic disorder characterized by intellectual disability and atypical behaviors. AS results from loss of expression of the E3 ubiquitin-protein ligase UBE3A from the maternal allele in neurons. Individuals with AS display impaired coordination, poor balance, and gait ataxia. PIEZO2 is a mechanosensitive ion channel essential for coordination and balance. Here, we report that PIEZO2 activity is reduced in *Ube3a* deficient male and female mouse sensory neurons, a human Merkel cell carcinoma cell line and female human iPSC-derived sensory neurons with *UBE3A* knock-down, and de-identified stem cell-derived neurons from individuals with AS. We find that loss of UBE3A decreases actin filaments and reduces PIEZO2 expression and function. A linoleic acid (LA)-enriched diet increases PIEZO2 activity, mechano-excitability, and improves gait in male AS mice. Finally, LA supplementation increases PIEZO2 function in stem cell-derived neurons from individuals with AS. We propose a mechanism whereby loss of *UBE3A* expression reduces PIEZO2 function and identified a fatty acid that enhances channel activity and ameliorates AS-associated mechano-sensory deficits.

Angelman syndrome (AS) is a neurogenetic disorder characterized by cognitive, motor, and behavioral abnormalities<sup>1</sup>. Individuals with AS display impaired motor coordination (e.g., unable to reach objects), abnormal gait (i.e., instability while walking), sensory ataxia, scoliosis, seizures, an abnormally happy disposition, and intellectual disability<sup>2–4</sup>. Likewise, AS mouse models have clearly defined phenotypes resembling behavioral dysfunction, such as ataxic gait, seizures, and learning deficits, making this model useful for testing therapeutics<sup>5–8</sup>. The AS phenotype results from the loss of expression of an E3 ubiquitin-protein ligase (*UBE3A*) from the maternal allele<sup>9–11</sup>.

*UBE3A* is regulated by genomic imprinting, a process that causes genes to be monoallelically expressed in neurons<sup>12</sup>. The cellular role of the UBE3A ubiquitin ligase is to transfer a single ubiquitin moiety from the E2 protein to a substrate protein<sup>13</sup>. UBE3A targets proteins for degradation, regulates their trafficking, and/or modulates their function<sup>14–16</sup>.

The abnormal gait associated with this disorder is debilitating, as most children have difficulty walking<sup>2</sup>. Importantly, gait (ataxic or broad-based) is among the most common behaviors (88%) observed in children with AS<sup>4</sup>. *UBE3A* is imprinted in most brain neurons<sup>1</sup>. For

<sup>1</sup>Department of Physiology, College of Medicine, University of Tennessee Health Science Center, Memphis, TN 38103, USA. <sup>2</sup>Integrated Biomedical Sciences Graduate Program, College of Graduate Health Sciences, Memphis, TN 38163, USA. <sup>3</sup>Department of Neurology, College of Medicine, University of Tennessee Health Science Center, Memphis, TN 38103, USA. <sup>4</sup>Department of Biochemistry and Molecular Biology, Faculty of Science and Technology, UPV/EHU, Leioa, Bizkaia, Spain. <sup>5</sup>School of Engineering and Sciences, Tecnológico de Monterrey, Ave. Eugenio Garza Sada 2501 Sur, Monterrey 64849, Mexico. <sup>6</sup>Anatomic Incorporated, Minneapolis, MN 55455, USA. <sup>7</sup>Ikerbasque, Basque Foundation for Science, Bilbao, Bizkaia, Spain. <sup>8</sup>Department of Anatomy and Neurobiology, College of Medicine, University of Tennessee Health Science Center, Memphis, TN 38104, USA. <sup>9</sup>Department of Pediatrics, College of Medicine, University of Tennessee Health Science Center, Memphis, TN 38104, USA. <sup>10</sup>These authors contributed equally: Luis O. Romero, Rebeca Caires.

e-mail: [vvasquez@uthsc.edu](mailto:vvasquez@uthsc.edu); [jcordero@uthsc.edu](mailto:jcordero@uthsc.edu)

instance, *UBE3A* exhibits maternal allele-specific expression in the Purkinje cell layer of the cerebellum and cell bodies of hippocampal CA1 – CA2 neurons in mice and humans<sup>17–19</sup>. Bruinsma et al. found that cerebellar function is only partly responsible for the behavioral deficits (e.g., ataxic-like gait, problems with balance) displayed by a mouse model of AS<sup>20</sup>. On the other hand, in the peripheral nervous system, it has been shown that proprioceptive and mechanosensitive dorsal root ganglia (DRG) neurons express the maternal *UBE3A* allele, while the paternal allele is silenced by an antisense transcript<sup>21</sup>. Hence, the loss of function of the maternal allele, in sensory neurons, could contribute to the phenotypes observed in AS.

Proprioception confers the ability to sense movement, tension, balance, and limb position<sup>22</sup>. The mechanosensitive ion channel PIEZO2 is expressed in sensory neurons innervating muscle spindles and Golgi tendon organs, where it mediates proprioception and balance<sup>23–26</sup>. A previous study demonstrated that *PIEZO2* deficiency in humans profoundly decreases proprioception, leading to sensory ataxia<sup>23</sup>. For example, a premature stop codon in *PIEZO2* causes unsteady gait and increased stride-to-stride variability in step length and force, among other deficits<sup>23,27</sup>. Likewise, mice lacking *Piezo2* display abnormal limb position and coordination, unstable gait, and balance deficits<sup>24,26,28</sup>. Moreover, *PIEZO2* is highly expressed in human Merkel cells and their afferent sensory neurons, where it mediates gentle touch and vibration<sup>29–32</sup>. Individuals carrying loss-of-function variants in *PIEZO2* have a selective loss of discriminative touch perception<sup>23</sup>. Similarly, mice deficient for *Piezo2* in the skin display reduced behavioral responses to gentle touch<sup>29,30,32</sup>.

The notable similarities between proprioception phenotypes in individuals with AS or *PIEZO2* loss of function (LOF) mutations, as well as their associated mouse models, raise the intriguing hypothesis that mechanotransduction could be impaired in AS. However, it is unclear if the loss of maternal *Ube3a* expression in DRG neurons affects *PIEZO2* activity. Here, we show that *PIEZO2* function is reduced in AS and that a safflower oil diet, enriched in linoleic acid (LA), increases *PIEZO2* activity, mechano-excitability, and ameliorates gait ataxia in a mouse model of AS.

## Results

### *Ube3a<sup>m-/p+</sup>* DRG neurons have decreased mechano-currents and -excitability

We used mice carrying a LOF *Ube3a* mutation on the C57BL/6 genetic background<sup>5</sup>. Heterozygous mice with a maternal deficiency (*Ube3a<sup>m-/p+</sup>*) display AS-associated phenotypes, including lack of balance and gait ataxia. Conversely, mice with a paternal deficiency (*Ube3a<sup>m+/p-</sup>*) do not show imbalance, unsteady gait, or sensory ataxia phenotypes<sup>5,6,33</sup>. Since mice lacking *Piezo2* experience severe mechanosensory and proprioceptive deficits<sup>24</sup>, we hypothesized that DRG neurons from the *Ube3a<sup>m-/p+</sup>* mice would display impaired mechanical responses. Parenthetically, ~ 80% of cultured mouse DRG neurons display mechanically activated currents<sup>34</sup>. These mechanocurrents display various inactivation kinetics (i.e., rapidly, intermediate, and slowly inactivating currents). The rapidly inactivating currents ( $\tau < 10$  ms) have been previously assigned to mouse *PIEZO2*<sup>35</sup>, whereas the intermediate ( $10 < \tau < 30$  ms) and slowly inactivating currents ( $\tau > 30$  ms) have not yet been identified.

We measured mechanocurrents in the whole-cell patch-clamp configuration from wild-type (WT), *Ube3a<sup>m-/p+</sup>*, and *Ube3a<sup>m+/p-</sup>* mouse DRG neurons. All experiments in this work were performed with male mice unless noted. All the mechanocurrents (including the rapidly inactivating currents assigned to *PIEZO2*) from the *Ube3a<sup>m-/p+</sup>* neurons were significantly reduced compared to WT or *Ube3a<sup>m+/p-</sup>* DRG neurons (Fig. 1a-b and Supplementary Fig. 1a-b). The displacement threshold required to elicit mechanocurrents in the *Ube3a<sup>m-/p+</sup>* neurons was slightly higher than WT or *Ube3a<sup>m+/p-</sup>* (Fig. 1c). The percentage of DRG neurons featuring *PIEZO2* mechanocurrents (i.e., rapidly inactivating

currents) was similar between WT, *Ube3a<sup>m-/p+</sup>*, and *Ube3a<sup>m+/p-</sup>* cultures (Supplementary Fig. 1c). Moreover, the capacitance distribution of recorded neurons was skewed towards medium to large diameter cells (i.e., mechanoreceptors<sup>36</sup>) and, importantly, was similar for WT, *Ube3a<sup>m-/p+</sup>*, and *Ube3a<sup>m+/p-</sup>* neurons (Supplementary Fig. 1d-e). Parenthetically, DRG neurons from female *Ube3a<sup>m-/p+</sup>* mice also displayed reduced mechanocurrents compared to WT or *Ube3a<sup>m+/p-</sup>* (Supplementary Fig. 1f-g). *PIEZO2* mediates most of the mechano-activated excitatory currents in mouse DRG neurons<sup>24,31</sup>. As neurons from *Ube3a<sup>m-/p+</sup>* mice display decreased mechanocurrents and an increase in displacement threshold, we sought to determine the ability of these neurons to elicit mechanically-activated action potentials. *Ube3a<sup>m-/p+</sup>* neurons required larger indentation steps to elicit action potentials than WT or *Ube3a<sup>m+/p-</sup>* ( $\geq 12$   $\mu$ m; Fig. 1d-e). Importantly, *Ube3a<sup>m-/p+</sup>* neurons have similar neuronal electrical excitability compared to WT neurons (membrane capacitance, action potential amplitudes, input resistances, and minimal current threshold required to elicit an action potential; Supplementary Fig. 1d, h-k). These results demonstrate that mechanocurrents (including those from *PIEZO2*) and mechano-excitability are reduced in *Ube3a<sup>m-/p+</sup>* DRG neurons.

### *UBE3A* knockdown alters the cytoskeleton and decreases *PIEZO2* function

We asked whether knocking down the expression of *UBE3A* in a human cell line by silencing RNA (siRNA) could recapitulate our findings in DRG neurons. *PIEZO2* is expressed in Merkel cells (tactile epithelial cells) and their innervating afferents, where it transduces skin indentation<sup>29,30,32</sup>. To support functional and biochemical experiments, we utilized the human Merkel cell carcinoma cell line (MCC13), in which *PIEZO2* mediates all endogenous mechanosensitive currents<sup>37</sup>. MCC13 cells displayed a decrease in *PIEZO2* currents after knocking down the expression of *UBE3A* or *PIEZO2*, when compared with mechanocurrents from the scrambled siRNA treatment (47% and 74%, respectively; Fig. 2a). We validated the siRNA treatment by performing RT-qPCR (Supplementary Fig. 2a-b). Quantification of mRNA levels demonstrates that knocking down *UBE3A* does not affect *PIEZO2* transcripts (Supplementary Fig. 2b). As expected, decreasing the mRNA levels of *UBE3A* reduced *UBE3A* protein expression (Supplementary Fig. 2c-d). Notably, knocking down the expression of *UBE3A* decreased 23% of *PIEZO2* membrane levels in MCC13 cells (Fig. 2b and Supplementary Fig. 2e). For electrophysiology experiments, we patched cells expressing the transfection marker siGLO green, whereas for western blots, we extracted membrane protein from a mixed culture of transfected and untransfected cells. This could explain the difference in effect size between currents and membrane protein expression reduction (47% vs. 23%). Conversely, *UBE3A* over-expression by transient transfection of *UBE3A* in MCC13 cells showed increased *PIEZO2* currents and membrane expression (Fig. 2c-d and Supplementary Fig. 2f). Taken together, in both mouse DRG neurons and human cell lines, downregulation of *UBE3A* expression decreases *PIEZO2* currents.

*Ube3a* deficient mice display reduced filamentous actin (F-actin) in cultured hippocampal neurons<sup>38</sup>. Moreover, using proteomic profiling, we have previously shown in *D. melanogaster* that *Ube3a* homozygous mutants have less F-actin, consistent with the identification of actin targets regulated by *Ube3a*<sup>39</sup>. *PIEZO1* and *PIEZO2* channel function is modulated by cytoskeletal elements<sup>40–43</sup>. We previously demonstrated that disrupting actin filaments with latrunculin A decreased *PIEZO2* currents in N2A cells<sup>42</sup>. Therefore, we tested the hypothesis that loss of *UBE3A* expression could decrease *PIEZO2* currents by impairing F-actin. MCC13 cells treated with latrunculin A display reduced *PIEZO2* currents compared to untreated cells (Fig. 2e). Of note, we measured a decrease in *PIEZO2* membrane expression levels in MCC13 cells after latrunculin A treatment, as well as a reduction in F-actin content (Fig. 2f and Supplementary Fig. 2g-i). Importantly,

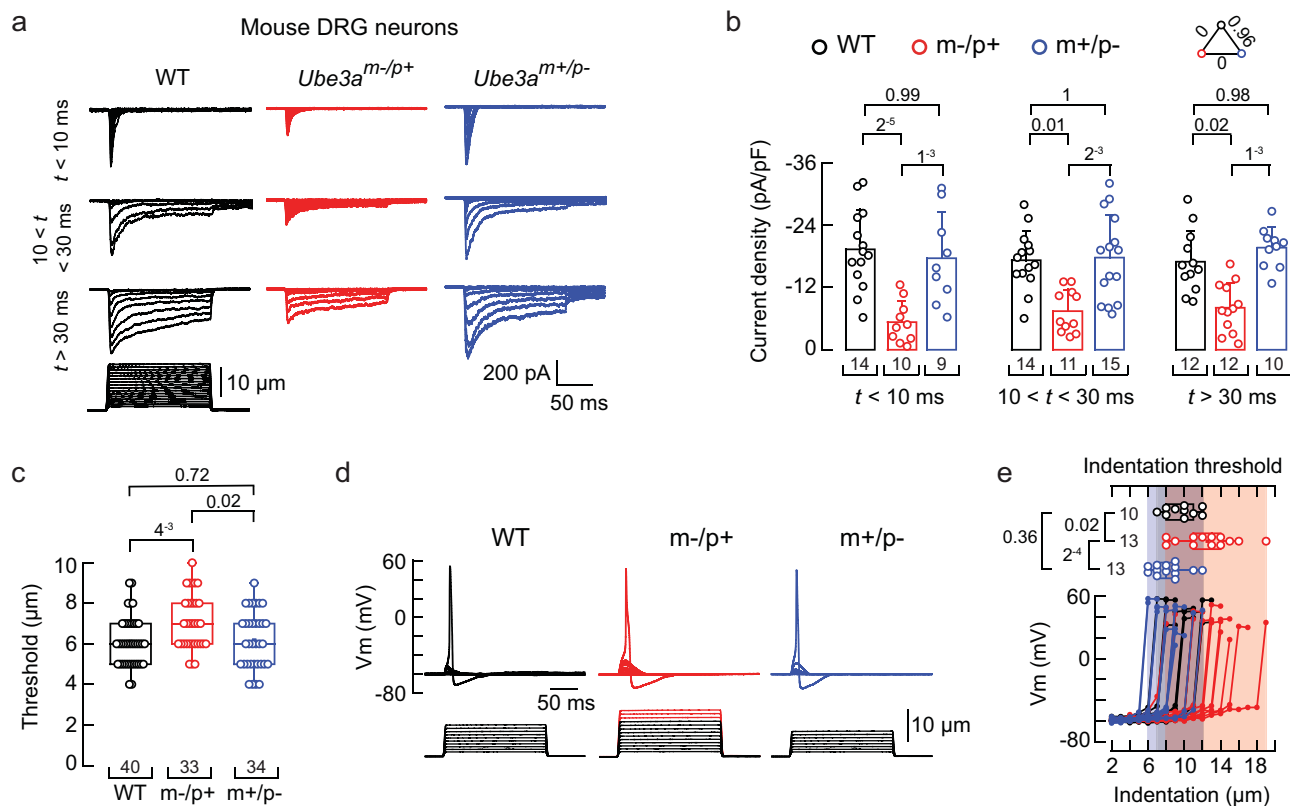


**Fig. 1 | *Ube3a<sup>m-/p+</sup>* DRG neurons display reduced mechano-currents and -excitability.** **a** Representative whole-cell patch-clamp recording elicited by mechanical stimulation ( $-60$  mV) of rapidly, intermediate, and slowly inactivating currents of WT, *Ube3a<sup>m-/p+</sup>*, and *Ube3a<sup>m+/p-</sup>* DRG neurons. **b** Current densities elicited by maximum displacement of DRG neurons classified by their time constant of inactivation. Bars are mean  $\pm$  SD. Two-way ANOVA ( $F = 35.44$ ,  $p = 2.63^{-12}$ ) and Tukey multiple-comparisons test. **c** Boxplots show the displacement thresholds required to elicit mechanocurrents of DRG neurons. Boxplots show mean (square), median (bisecting line), bounds of box (75<sup>th</sup> to 25<sup>th</sup> percentiles), outlier range with 1.5 coefficient (whiskers), and minimum and maximum data points. Kruskal-Wallis

( $H = 9.51$ ;  $p = 0.0086$ ) and Dunn's multiple comparisons test. **d** Representative current-clamp recordings of membrane potential changes elicited by mechanical stimulation in DRG neurons. **e** Membrane potential peak vs. mechanical indentation of independent mouse DRG neurons. At the top, boxplots show the displacement threshold required to elicit an action potential in these neurons. Boxplots show mean (square), median (bisecting line), bounds of box (75<sup>th</sup> to 25<sup>th</sup> percentiles), outlier range with 1.5 coefficient (whiskers), and minimum and maximum data points. One-way ANOVA ( $F = 10.54$ ;  $p = 2.89^{-4}$ ) and Tukey multiple-comparisons test.  $n$  is denoted in each panel. Post hoc  $p$  values are denoted in the corresponding panels. Source data are provided as a Source Data file.

we also observed a reduction in actin content after knocking down the expression of *UBE3A* in MCC13 cells (Fig. 2g and Supplementary Fig. 2j). Our data support that knocking down *UBE3A* expression reduces actin filaments, leading to a decrease in PIEZO2 membrane expression and currents.

*UBE3A* could alter actin dynamics by regulating the content of actin-binding protein(s). Cofilin is an actin-binding protein that promotes rapid actin filament disassembly<sup>44</sup>. We determined an increase in cofilin content after knocking down the expression of *UBE3A* in MCC13 cells (Fig. 2h and Supplementary Fig. 2k). Moreover, over-expression of cofilin in MCC13 cells, by transient transfection, decreased PIEZO2 currents compared to control cells (Fig. 2i). Previous works have shown that cofilin can be ubiquitinated by the E3 ubiquitin ligases Cbl and AIP4<sup>45</sup>; however, whether *UBE3A* ubiquitinates cofilin is unknown. Using a stringent cell-culture based ubiquitination assay<sup>46,47</sup>, we demonstrated that cofilin ubiquitination is increased by WT *UBE3A* but not by a ligase dead (LOF) version of this E3 enzyme (Fig. 2j and Supplementary Fig. 2l). Our findings support a model whereby loss of *UBE3A* expression increases cofilin, which severs actin filaments and decreases PIEZO2 membrane expression and currents.

#### *Ube3a<sup>m-/p+</sup>* DRG neurons display reduced F-actin, and promoting actin polymerization increases PIEZO2 currents

Based on our findings in MCC13 cells, we reasoned that *Ube3a<sup>m-/p+</sup>* mouse DRG neurons could have a reduced F-actin content. Indeed,

cultured *Ube3a<sup>m-/p+</sup>* neurons fixed and stained with Alexa Fluor 488 phalloidin (selective actin filament stain) displayed a reduced mean fluorescence intensity compared to WT (Fig. 3a). This result is further supported by the increase in the G/F actin ratio in *Ube3a<sup>m-/p+</sup>* DRG neurons, as determined by western blots (Fig. 3b and Supplementary Fig. 3a). Jasplakinolide is a peptide that promotes actin polymerization and stabilizes actin filaments<sup>48</sup>. Notably, jasplakinolide treatment significantly increased PIEZO2 currents in *Ube3a<sup>m-/p+</sup>* mouse DRG neurons (Fig. 3c). An increase in cofilin could account for the decrease in actin in the *Ube3a<sup>m-/p+</sup>* mouse DRG neurons. We found elevated levels of cofilin (a target of *UBE3A*) in *Ube3a<sup>m-/p+</sup>* mouse DRG neurons when compared to neurons from WT mice (Fig. 3d and Supplementary Fig. 3b). Importantly, knocking down the expression of *cofilin* in *Ube3a<sup>m-/p+</sup>* DRG neurons increases PIEZO2 currents similar to WT levels (Fig. 3e). Taken together, our results demonstrate that *Ube3a<sup>m-/p+</sup>* DRG neurons have an impaired actin cytoskeleton and treatments that stabilize actin filaments or reduce cofilin expression increase PIEZO2 function.

#### Linoleic acid increases PIEZO2 currents

There are no agonists available for PIEZO2<sup>49</sup>. We have previously shown that PIEZO1 (a close homolog of PIEZO2) displayed slower inactivation and more mechanocurrents in plasma membranes containing high levels of linoleic acid (LA,  $\omega$ -6 C18:2)<sup>50</sup> and Supplementary Fig. 4a. Considering the similarities between the PIEZO channels,

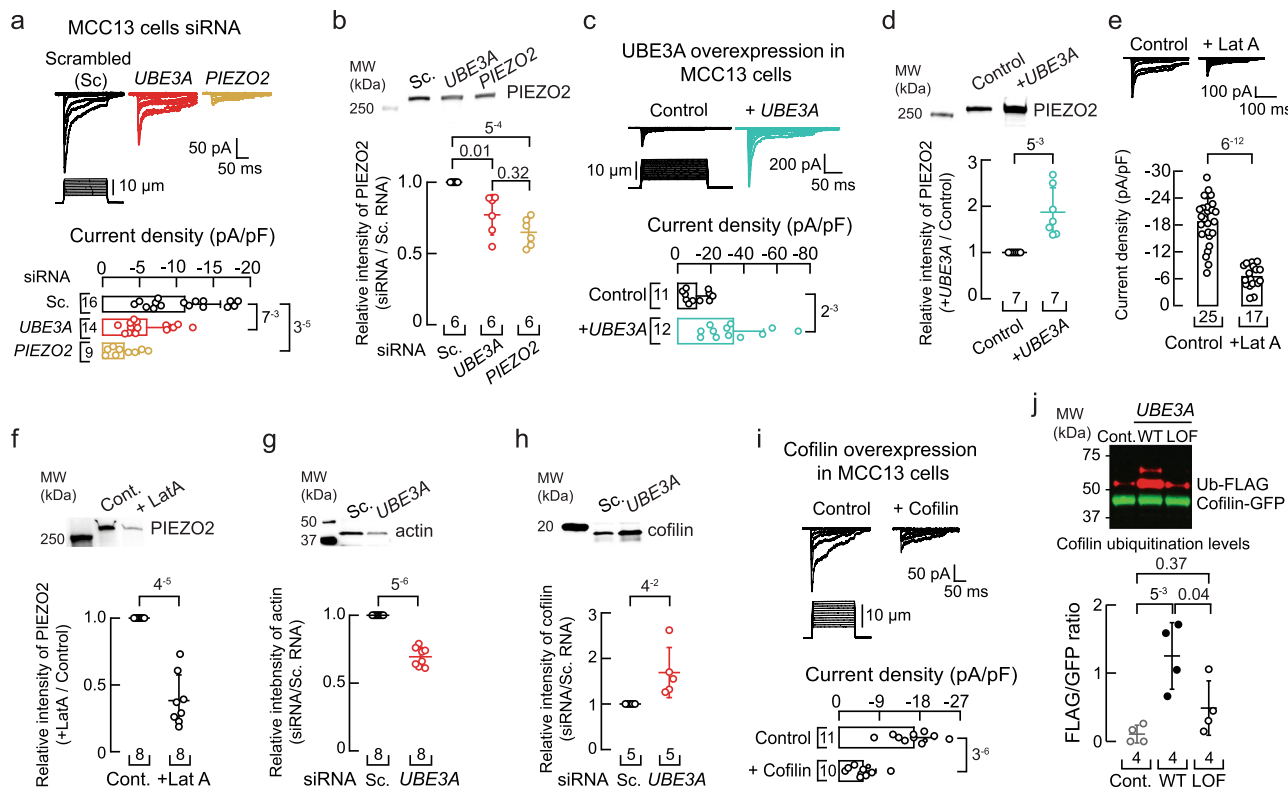


**Fig. 2 | UBE3A knockdown increases cofilin and decreases F-actin content and PIEZO2 function.** **a**, Top, representative whole-cell patch-clamp recordings of currents elicited by mechanical stimulation ( $-60$  mV) in MCC13 cells transfected with scrambled, *UBE3A*, or *PIEZO2* siRNAs. Bottom, current densities elicited by maximum displacement of siRNA-transfected cells. Bars are mean  $\pm$  SD. Kruskal-Wallis ( $H = 18.76$ ;  $p = 8.4^{-5}$ ) and Dunn's multiple comparisons test. **b**, Top, western blot (anti-*PIEZO2*) of the membrane fractions of MCC13 cells transfected as in (a). Bottom, mean/scatter-dot plot showing relative intensities of *PIEZO2* protein normalized to *PIEZO2* in the Sc. group. Lines are mean  $\pm$  SD. Kruskal-Wallis ( $H = 12.78$ ;  $p = 0.0017$ ) and Dunn's multiple comparisons test. **c**, Top, currents elicited by mechanical stimulation ( $-60$  mV) in cells transfected with *UBE3A* plasmid. Bottom, current densities elicited by maximum displacement of *UBE3A* transfected cells. Bars are mean  $\pm$  SD. Two-tailed unpaired *t*-test with Welch's correction ( $t = 3.9$ ). **d**, Top, western blot (anti-*PIEZO2*) of the membrane fractions of MCC13 cells transfected with *UBE3A* plasmid. Bottom, mean/scatter-dot plot showing relative intensities of *PIEZO2* protein in *UBE3A* transfected cells normalized to *PIEZO2* in the control group. Lines are mean  $\pm$  SD. Two-tailed one-sample *t*-test ( $t = 4.4$ ). **e**, Top, currents elicited by mechanical stimulation ( $-60$  mV) of latrunculin A (1  $\mu$ M; 24 h)-treated MCC13 cells. Bottom, current densities elicited by maximum displacement. Bars are mean  $\pm$  SD. Two-tailed unpaired *t*-test with Welch's correction ( $t = 9.9$ ). **f**, Top, western blot (anti-*PIEZO2*) of the membrane fractions of MCC13 cells treated

as in (e). Bottom, mean/scatter-dot plot showing relative intensities of *PIEZO2* protein normalized to *PIEZO2* in the control group. Lines are mean  $\pm$  SD. Two-tailed one-sample *t*-test ( $t = -9.1$ ). **g**, Top, western blot (anti-actin) of the cytoskeletal fractions of MCC13 transfected with scrambled (Sc.) or *UBE3A* siRNAs. Bottom, mean/scatter-dot plot showing relative intensities of actin protein normalized to actin in the Sc. group. Lines are mean  $\pm$  SD. Two-tailed one-sample *t*-test ( $t = -12.5$ ). **h**, Top, western blot (anti-cofilin) of the cytosolic fractions of MCC13 transfected as in (g). Bottom, mean/scatter-dot plot showing relative intensities of cofilin protein normalized to cofilin in the Sc. group. Lines are mean  $\pm$  SD. Two-tailed one-sample *t*-test ( $t = 2.8$ ). **i**, Top, currents elicited by mechanical stimulation ( $-60$  mV) in MCC13 cells transfected with *cofilin* plasmid. Bottom, current densities elicited by maximum displacement of *cofilin* transfected cells. Bars are mean  $\pm$  SD. Two-tailed unpaired *t*-test with Welch's correction ( $t = 6.8$ ). **j**, Top, western blot of pulldown GFP-tagged cofilin from HEK293T cells transfected with a control vector (Ctrl), wild-type *UBE3A* (WT), or a catalytically inactive *UBE3A* (LOF). The ubiquitinated (Ub) fraction (red) was monitored with an anti-FLAG antibody. Bottom, mean/scatter-dot plot showing Ub-FLAG/Cofilin-GFP ratios. Lines are mean  $\pm$  SD. One-way ANOVA ( $F = 9.86$ ;  $p = 0.0054$ ) and Tukey multiple-comparisons test.  $n$  is denoted in each panel. Post hoc  $p$ -values are denoted in the corresponding panels. Source data are provided as a Source Data file.

we tested the ability of LA to enhance *PIEZO2* function. To this end, we transfected *Piezo2* variant 14 (abundant in the mouse trigeminal ganglion)<sup>51</sup> into N2A cells lacking *Piezo1* (*Piezo1*<sup>-/-</sup> N2A cells)<sup>52</sup> to distinguish the effect of LA on *PIEZO2* gating unequivocally. *PIEZO2* mechanocurrents were measured after supplementing the cell media overnight with 100  $\mu$ M LA. Supplementation with LA increased *PIEZO2* currents twofold ( $-50.09 \pm 19.84$  pA/pF vs.  $-106.32 \pm 58.9$  pA/pF, mean  $\pm$  SD) (Fig. 4a-b and Supplementary Fig. 4b). Overnight incubation with LA increased (~sevenfold) the plasma membrane content of this PUFA, as determined by liquid chromatography-mass spectrometry (LC-MS; Supplementary Fig. 4c). Next, we tested fatty acids of varying acyl-chain length and unsaturations to assess the chemical and structural bases whereby LA increases *PIEZO2* function. We did not observe an increase in *PIEZO2* activity for stearic acid (SA; C18:0), oleic acid (OA; C18:1),  $\omega$ -6 PUFAs downstream of LA [gamma linolenic acid

( $\gamma$ LA; C18:3), dihomo gamma-linolenic acid (DyLA; C20:3), arachidonic acid (AA; C20:4), docosatetraenoic acid (DTA; 22:4], or  $\omega$ -3 PUFAs ( $\alpha$ LA; C18:3 and DHA; C22:6) (Fig. 4a-b and Supplementary Fig. 4d-e). Additionally, LA slowed *PIEZO2* channel inactivation in *Piezo1*<sup>-/-</sup> N2A cells (Fig. 4a and c). These results support that LA (C18:2), but not the other fatty acids tested, enhances *PIEZO2* activity.

Similar to *Piezo1*<sup>-/-</sup> N2A cells, we measured a significant increase in endogenous *PIEZO2* currents in MCC13 cells after overnight supplementation with LA, in a dose-dependent manner (Fig. 4d-e and Supplementary Fig. 4f). We also used an alternative supplementation protocol to add lower doses of LA for several days. Supplementing MCC13 cells with 20  $\mu$ M LA each day, for five days, significantly increased *PIEZO2* currents (Fig. 4d-e). These concentrations are within the range of circulating fatty acids present in the blood plasma of healthy adults<sup>53</sup>. Our results

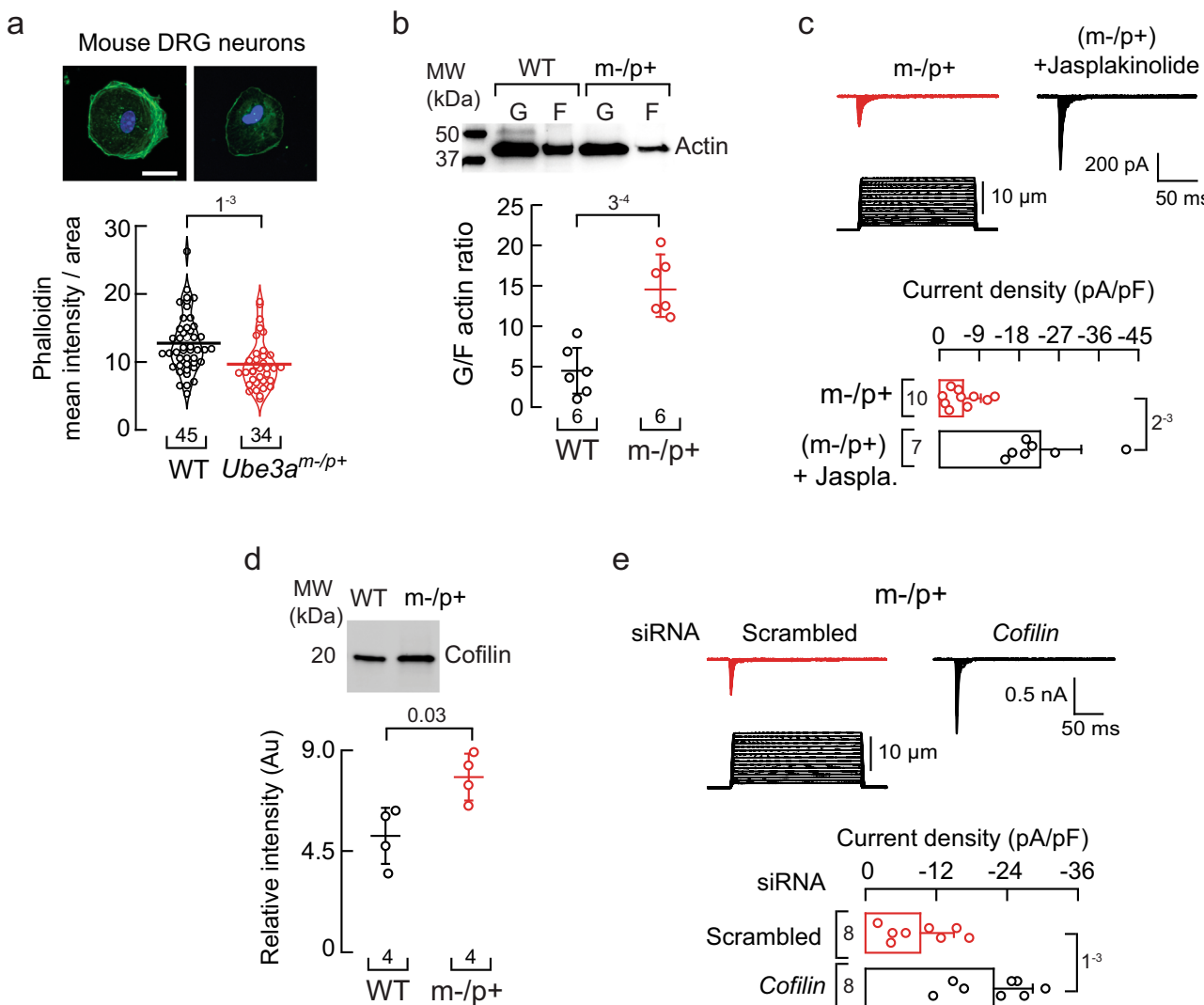


**Fig. 3 | *Ube3a*<sup>m/p+</sup> DRG neurons display reduced F-actin and jasplakinolide treatment increases PIEZO2 currents.** **a**, Top, representative micrographs of cultured WT and *Ube3a*<sup>m/p+</sup> DRG neurons fixed and stained with phalloidin (green) and DAPI (blue). Scale bar 20 μm. Bottom, phalloidin mean intensity normalized by the neuron's area is depicted as a violin plot with the means shown as horizontal bars. Two-tailed unpaired t-test ( $t = 3.41$ ). **b**, Top, western blot of soluble and insoluble actin (G and F, respectively) of WT and *Ube3a*<sup>m/p+</sup> DRGs. Bottom, mean/scatter-dot plot showing G/F actin ratios. Lines are mean ± SD. Two-tailed unpaired t-test ( $t = 5.43$ ). **c**, Top, representative whole-cell patch-clamp recordings of PIEZO2 currents elicited by mechanical stimulation (-60 mV) of control and jasplakinolide (0.5 μM; 18 h)-treated *Ube3a*<sup>m/p+</sup> DRG neurons. Bottom, current densities elicited by maximum displacement. Bars are mean ± SD. Two-tailed unpaired t-test with Welch's correction ( $t = 4.68$ ). **d**, Top, representative western blot (anti-cofilin) of the cytosolic fractions of WT and *Ube3a*<sup>m/p+</sup> DRGs. Bottom, mean/scatter-dot plot showing relative intensities of cofilin content. Lines are mean ± SD. Two-tailed Mann-Whitney test ( $U = 0$ ). **e**, Top, representative whole-cell patch-clamp recordings of currents elicited by mechanical stimulation (-60 mV) of *Ube3a*<sup>m/p+</sup> DRG neurons transfected with scrambled or *cofilin* siRNAs. Bottom, current densities elicited by maximum displacement of siRNA-transfected *Ube3a*<sup>m/p+</sup> DRGs. Bars are mean ± SD. Two-tailed unpaired t-test ( $t = 4.02$ ). n is denoted in each panel. Post-hoc p-values are denoted in the corresponding panels. Source data are provided as a Source Data file.

by maximum displacement. Bars are mean ± SD. Two-tailed unpaired t-test with Welch's correction ( $t = 4.68$ ). **d**, Top, representative western blot (anti-cofilin) of the cytosolic fractions of WT and *Ube3a*<sup>m/p+</sup> DRGs. Bottom, mean/scatter-dot plot showing relative intensities of cofilin content. Lines are mean ± SD. Two-tailed Mann-Whitney test ( $U = 0$ ). **e**, Top, representative whole-cell patch-clamp recordings of currents elicited by mechanical stimulation (-60 mV) of *Ube3a*<sup>m/p+</sup> DRG neurons transfected with scrambled or *cofilin* siRNAs. Bottom, current densities elicited by maximum displacement of siRNA-transfected *Ube3a*<sup>m/p+</sup> DRGs. Bars are mean ± SD. Two-tailed unpaired t-test ( $t = 4.02$ ). n is denoted in each panel. Post-hoc p-values are denoted in the corresponding panels. Source data are provided as a Source Data file.

demonstrate that the essential dietary fatty acid LA (C18:2) increases PIEZO2 activity.

#### LA increases membrane structural disorder

Western blot analyses revealed that LA supplementation did not increase PIEZO2 membrane expression in MCC13 cells (Fig. 5a-b). Furthermore, perfusion of free LA (150 μM) onto *Piezo1*<sup>-/-</sup> N2A cells transfected with PIEZO2 did not change channel function (Fig. 5c-d). Hence, it is possible that LA increases PIEZO2 function by modifying the membrane's mechanical properties. To determine the effect of LA on membranes, we used differential scanning calorimetry (DSC) and measured changes in the heat-capacity profiles (Cp) of synthetic membranes (1,2-dipalmitoyl-sn-glycero-3-phosphocholine, DPPC) containing various fatty acids. From the DSC thermograms, we obtained melting transition temperature (Tm) and cooperativity (κ) as

a readout of both lipid-lipid interaction and membrane organization (Fig. 5e)<sup>54,55</sup>. LA displayed the lowest melting temperature (i.e., less temperature required to transition from the gel to the liquid phase) compared to DPPC alone or liposomes containing SA, OA, γLA, DγLA, AA, or DTA (Fig. 5e-f). This result indicates that LA elicits the largest increase in membrane structural disorder. We also determined that liposomes containing LA display the largest cooperative unit, indicating that there are more lipids undergoing the phase transition simultaneously (Fig. 5g). The effect of LA versus the other fatty acids is made further apparent when plotting the current densities (from Fig. 4b) as a function of cooperativity (Pearson's r: 0.93; Fig. 5h).

Next, we tested the effect of LA supplementation on the bacterial mechanosensitive ion channel of large conductance (MsCl), whose gating relies solely on the mechanical properties of the plasma membrane<sup>56</sup>. To this end, we measured pressure-activated currents

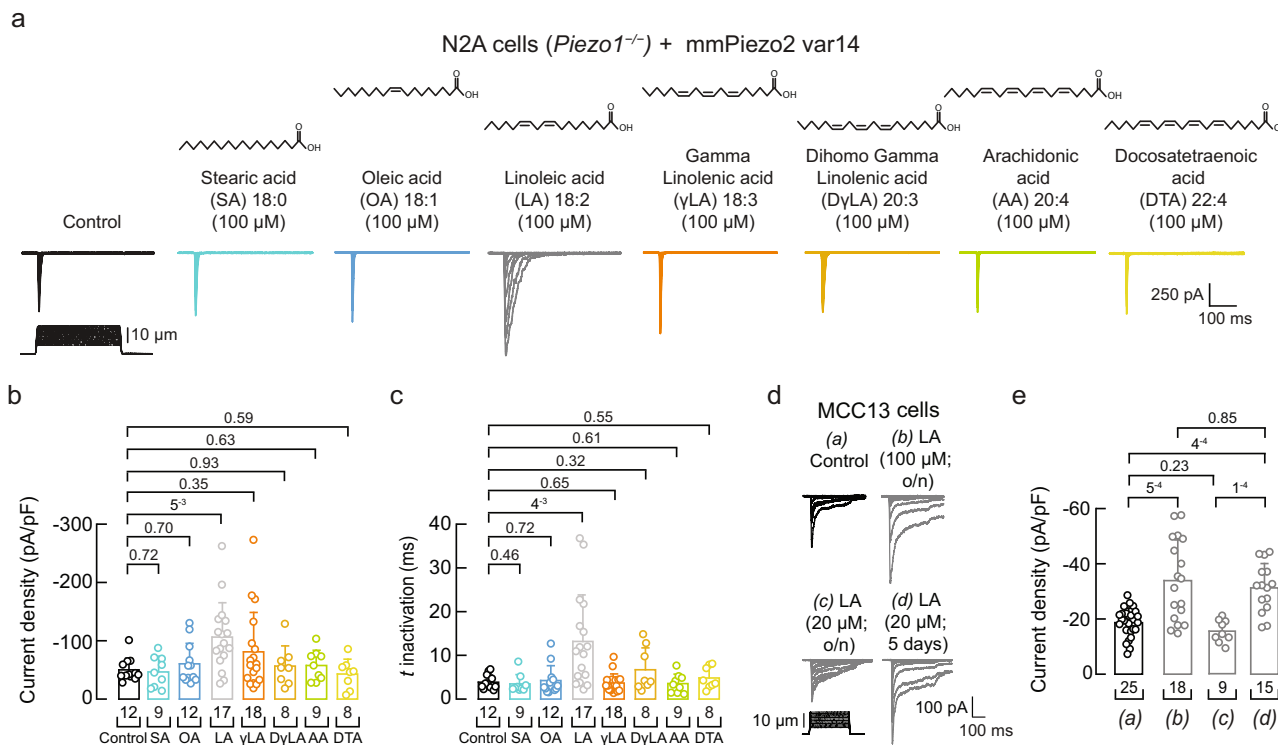


**Fig. 4 | LA increases PIEZO2 activity in *Piezo1*<sup>-/-</sup> N2A and MCC13 cells.**

a Representative whole-cell patch-clamp recordings of currents elicited by mechanical stimulation ( $-60$  mV) in control, SA, OA, LA,  $\gamma$ LA, D $\gamma$ LA, AA, and DTA (100  $\mu$ M; 24 h)-treated *Piezo1*<sup>-/-</sup> N2A cells transfected with *Piezo2* variant 14 (var14).

b Current densities elicited by maximum displacement of control or fatty acid-treated *Piezo1*<sup>-/-</sup> N2A cells transfected with *Piezo2* var14. Bars are mean  $\pm$  SD.

Kruskal-Wallis ( $H = 15.7$ ;  $p = 0.028$ ) and Dunn's multiple comparisons test. c Time constants of inactivation elicited by maximum displacement of control or fatty acid-treated *Piezo1*<sup>-/-</sup> N2A cells transfected with *Piezo2* var14. Bars are mean  $\pm$  SD.

Kruskal-Wallis ( $H = 22.41$ ;  $p = 0.0022$ ) and Dunn's multiple comparisons test.

d Representative whole-cell patch-clamp recordings elicited by mechanical stimulation ( $-60$  mV) of (a) control, (b) LA (100  $\mu$ M; o/n), (c) LA (20  $\mu$ M; o/n), and (d) LA (20  $\mu$ M each day for five days)-treated MCC13 cells.

e Current densities elicited by maximum displacement of control and LA-treated MCC13 cells. Bars are mean  $\pm$  SD. Kruskal-Wallis ( $H = 27.03$ ;  $p = 5.8^{-6}$ ) and Dunn's multiple comparisons test. n is denoted in each panel. Post hoc p-values are denoted above the bars. Source data are provided as a Source Data file.

of MscL transfected in *Piezo1*<sup>-/-</sup> N2A cells, with or without LA. Similar to what has been reported for MscL reconstituted in liposomes containing LA<sup>57</sup>, supplementing N2A cells with this fatty acid increased the function of MscL, when compared to untreated cells, as determined by the leftward shift in the pressure required to open the channel (Fig. 5i-j). Taken together, these results support the notion that the effect of LA on increasing PIEZO2 function is likely through membrane remodeling (i.e., higher membrane fluidity and cooperativity) rather than changes in protein expression or the interaction of free LA with the channel.

#### Linoleic acid supplementation increases mechanocurrents in *Ube3a*<sup>m-/p+</sup> DRG neurons

We tested whether LA could increase mechano-responses in DRG neurons dissected and cultured from *Ube3a*<sup>m-/p+</sup> mice. The culture media was supplemented with LA (50  $\mu$ M for the first 24 h, followed by 100  $\mu$ M for the second 24 h period) for two days before measuring currents. A two-day supplementation protocol improved neuronal viability and the ability to perform patch-clamp recordings. Like DRG neurons measured after 24 h (Fig. 1b), *Ube3a*<sup>m-/p+</sup> DRG neurons displayed reduced mechanocurrents compared with WT or *Ube3a*<sup>m+/p-</sup> DRG neurons, after 48 h in culture (Supplementary Fig. 5a). Notably, LA supplementation increased all the mechanocurrents in cultured DRG neurons from WT, *Ube3a*<sup>m+/p+</sup>, and *Ube3a*<sup>m-/p-</sup> mice (Fig. 6a-d and Supplementary Fig. 5b). *Ube3a*-deficient neurons supplemented with LA displayed a decrease in the displacement threshold required to elicit mechanocurrents when compared to control, whereas no effect was measured for WT and *Ube3a*<sup>m+/p-</sup> neurons (Fig. 6e).

Parenthetically, we found that DRG neurons supplemented with LA have similar membrane capacitance, action potential amplitudes, resting potentials, input resistances, and minimal current threshold required to elicit an action potential, compared to control neurons (Supplementary Fig. 5c-h), suggesting that LA does not affect neuronal electrical excitability. Additionally, LA supplementation does not alter the function of the sensory receptors TRPV1, TRPA1, and TRPM8 (Supplementary Fig. 5i-n). Together, these results demonstrate that LA increases mechanocurrents, including those from PIEZO2, while decreasing the mechanical threshold for *Ube3a*<sup>m-/p+</sup> DRG neurons.

#### A linoleic acid-enriched diet recovers *Ube3a*<sup>m-/p+</sup> neuronal mechanocurrents and -excitability

LA is an essential  $\omega$ -6 fatty acid and a structural component of plasma membranes<sup>58</sup>. It is commonly found in safflower, soybean, sunflower, corn, and canola oils<sup>59–61</sup>. Since LA supplementation in the culture media increases mechanocurrents, we postulated that including LA in the animal's diet may rescue the mechano-deficits of *Ube3a*<sup>m-/p+</sup> DRG neurons. To this end, we used a non-western-style diet enriched in safflower oil as a delivery method to increase LA in DRG neurons. Oil from the seeds of the safflower plant has been shown to contain over 70% LA<sup>62</sup>. LA can accumulate when its consumption in the diet is increased due to its limited conversion by the delta-6 desaturase enzyme<sup>59</sup>. We pair-fed *Ube3a*<sup>m-/p+</sup> mice for 12 weeks with a LA-enriched diet and found that their DRG neurons had higher LA membrane content (-twofold) when compared to WT and *Ube3a*<sup>m+/p+</sup> mice fed with a standard diet (Fig. 7a), as determined by LC-MS. On the other hand, the content of downstream

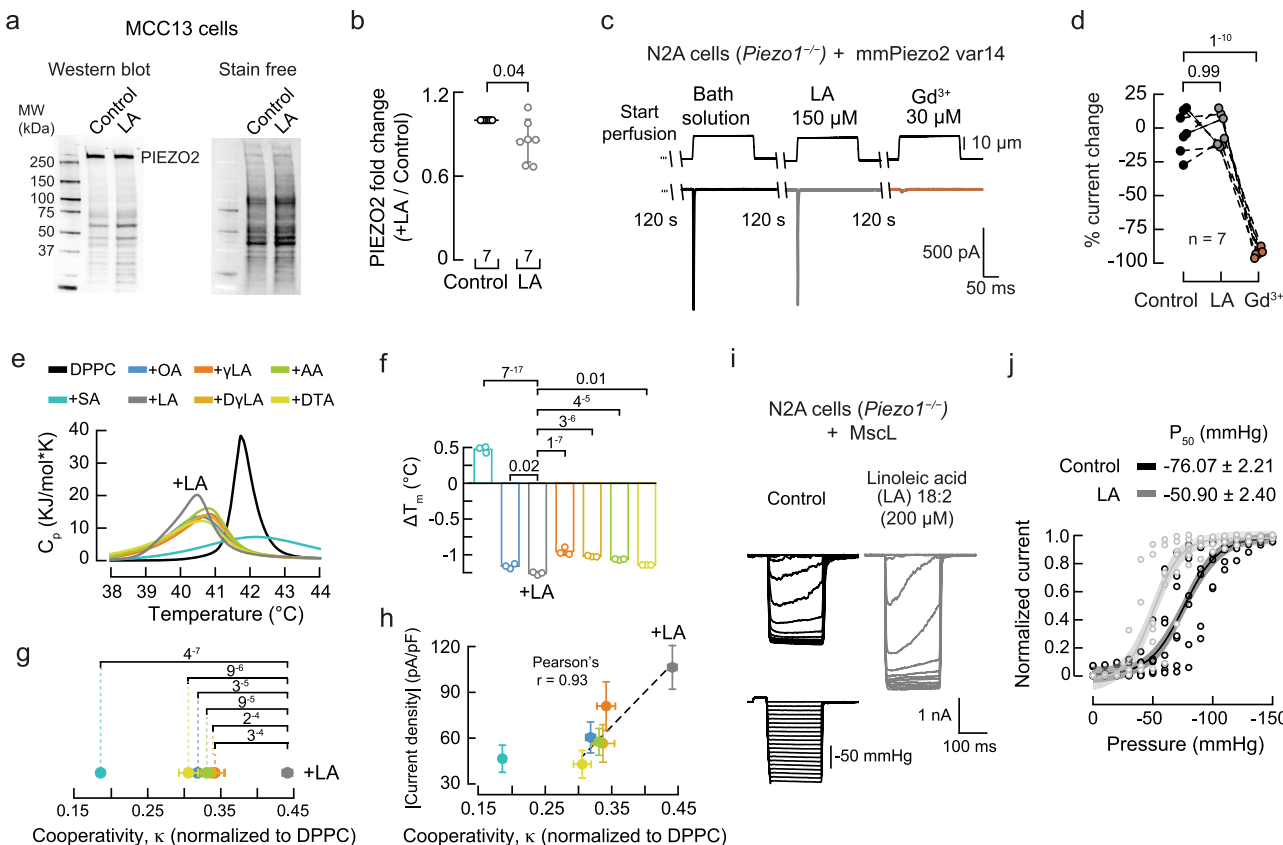


**Fig. 5 | LA does not increase PIEZO2 expression but alters the physical properties of the membranes.** **a** Western (anti-PIEZO2) and stain-free blots of the membrane fractions of control and LA-treated MCC13 cells. **b** Mean/scatter-dot plot showing relative intensities of PIEZO2 protein normalized to the level of PIEZO2 in the control group. Lines are mean  $\pm$  SD. Two-tailed one-sample *t*-test (*t* = -2.5). **c** Representative currents elicited by 10  $\mu$ m displacement of *Piezo2* var14 transfected cells after perfusing bath solution with LA and Gd<sup>3+</sup>. **d** Percent current change from independent cells recorded with the protocol shown in (c). Paired data points represent individual cells. One-sided repeated measures ANOVA (*F* = 186.94; *p* = 9.51<sup>-6</sup>) and Tukey test. **e** Thermotropic characterization of the DPPC/fatty acid systems using DSC: control ( $T_m$  = 41.75  $\pm$  0.05 °C; mean  $\pm$  sd), SA (42.23  $\pm$  0.04 °C), OA (40.59  $\pm$  0.03 °C), LA (40.53  $\pm$  0.06 °C), γLA (40.80  $\pm$  0.05 °C), DyLA (40.73  $\pm$  0.01 °C), AA (40.79  $\pm$  0.01 °C), and DTA (40.61  $\pm$  0 °C). **f** Effects of DPPC/fatty acids on melting temperatures ( $\Delta T_m$ ) with respect to DPPC membranes. *n* = 3. Bars

are mean  $\pm$  SD. One-way ANOVA (*F* = 1,177; *p* = 0) and Bonferroni test. **g** Cooperative unit ( $\kappa$ ) of the main transition of DPPC/fatty acid systems extracted from the thermotropic curves shown in (e), normalized to DPPC. Circles are mean  $\pm$  SD. *n* = 3. Two-way ANOVA (*F* = 45.7689; *p* = 2.09<sup>-8</sup>) and Tukey multiple-comparisons test. **h** Mean current densities of control or fatty acid-treated *Piezo1<sup>-/-</sup>* N2A cells transfected with *Piezo2* var14 vs. the cooperative unit ( $\kappa$ ) of the main transition of DPPC/fatty acid systems. Circles are mean  $\pm$  SEM. *n* = 3. A Pearson correlation was fitted to the unsaturated fatty acids data. **i** Inside-out recordings of currents elicited by negative pressure (at -10 mV) in LA (200  $\mu$ M; 24 h)-treated cells transfected with Mscl. **j** Normalized current responses to pressure changes of control (*n* = 7) and LA (200  $\mu$ M; 24 h; *n* = 6)-treated cells transfected with Mscl. A Boltzmann function was fitted to the data (continuous lines). The shadows indicate the 95% confidence bands. *n* is denoted in each panel. Post-hoc *p*-values are denoted in the corresponding panels. Source data are provided as a Source Data file.

PUFAs (γLA, DyLA, AA, and DTA) remained constant (Supplementary Fig. 6a). Remarkably, cultured DRG neurons from *Ube3a<sup>m-/p+</sup>* mice fed with a LA-enriched diet displayed robust mechanocurrents and a lower displacement threshold when compared to neurons from *Ube3a<sup>m-/p+</sup>* mice fed with standard or high-fat diets (Fig. 7b-d and Supplementary Fig. 6b). Although the LA-enriched diet enhanced PIEZO2- and intermediate inactivating mechanocurrents, it had no effect on those that were slowly inactivating (Fig. 7c, right panel). However, further supplementing DRG neurons from *Ube3a<sup>m-/p+</sup>* mice fed with a LA-enriched diet with additional LA (during culture) increased the slowly inactivating currents (Supplementary Fig. 6c-d). Next, we tested DRG neurons of the *Ube3a<sup>m-/p+</sup>* mice fed with a LA-enriched diet for their ability to elicit mechanically activated action potentials. These neurons required smaller indentation steps ( $\leq$ 10  $\mu$ m, like WT and *Ube3a<sup>m+/p+</sup>* mice) to elicit action potentials compared to neurons from *Ube3a<sup>m-/p+</sup>* mice on standard or high-fat diets ( $\geq$ 12  $\mu$ m; Fig. 7e-f).

We also tested the effect of a LA-enriched diet on WT animals and found that LA increased PIEZO2 currents in neurons compared to those from animals fed with a standard diet, but did not change the displacement threshold or threshold for mechanically activated action

potentials (Supplementary Fig. 6e-i). Of note, WT, *Ube3a<sup>m-/p+</sup>* mice fed with a standard diet, and *Ube3a<sup>m-/p+</sup>* mice fed with a LA-enriched diet had similar body weights after pair-feeding (Supplementary Fig. 7a). Furthermore, *Ube3a<sup>m-/p+</sup>* mice fed with a LA-enriched diet displayed similar behavioral responses to noxious mechanical (pinprick and tail clip) and thermal stimuli (hot plate and Hargreaves), suggesting that a LA-enriched diet does not enhance nociception (Supplementary Fig. 7b-e). We also determined that feeding the LA-enriched diet to *Ube3a<sup>m-/p+</sup>* mice did not alter their cytokine profile compared to those fed with the control diet, indicating that the non-western safflower oil-enriched diet does not induce inflammation (Supplementary Fig. 7f). These results demonstrate that a LA-enriched diet increases mechanocurrents, including those from PIEZO2, and is sufficient to recover the mechanical excitability of *Ube3a<sup>m-/p+</sup>* DRG neurons.

#### A linoleic acid-enriched diet ameliorates gait ataxia in a mouse model of AS

We sought to determine the effect of the LA-enriched diet on the gait of *Ube3a<sup>m-/p+</sup>* mice. Mouse gait measurements are consistent, commonly used to assess locomotion in several human disease models,